Available online at www.sciencedirect.com
SCIENCE DIRECT®
Journal of Sound and Vibration 272 (2004) 287–299
JOURNAL OF SOUND AND VIBRATION
www.elsevier.com/locate/jsvi

Investigation of thrust effect on the vibrational characteristics of flexible guided missiles

S.H. Pourtakdoust*, N. Assadian

Department of Aerospace Engineering, Sharif University of Technology, Azadi Street, Tehran 11365 8639, Iran

Received 18 July 2002; accepted 14 March 2003

Abstract

In this paper the effect of thrust on the bending behaviour of flexible missiles is investigated. For this purpose, the governing equations of motion of a flexible guided missile are derived following the Lagrangian approach. The missile is idealized as a non-uniform beam where the bending elastic deflections are modelled using the method of modal substitution. The vehicle (time varying) bending modeshapes and natural frequencies are determined by modelling variable mass and stiffness distributions with thrust and mass burning effects accounted for. To solve this problem the missile is divided into several segments of uniform stiffness, density and axial force distribution. This approach produces a non-linear transcendental equation, which requires an iterative scheme to numerically determine the magnitude of the eigenvalues. Since inertial measuring units (IMU) also sense the local body vibrations, the mass and stiffness non-uniformities plus the thrust action on elastic missiles can potentially influence their measurements and thus must be properly accounted for in an aeroelastic simulation. It is noted that the thrust force reduces the vehicle natural frequency while mass consumption increases it. Thus the modal natural frequencies can either decrease or increase in time. Also the critical buckling thrust, which dynamically causes a zero natural frequency, is obtained and therefore the thrust instability limitations are determined through simulation. With proper modelling of the IMU vibrations effects and engine/thrust fluctuations, the influence of body vibrations on the missile dynamics and controls are investigated with axial thrust effect.

1. Introduction

Development of science and technology in large rockets and missiles has led to bigger values of thrust-to-weight and length-to-diameter ratios required for long range flights. Since the drag force is proportional to the square of the missile diameter, one prefers to vary the length rather than the

*Corresponding author. Tel./fax: +98-21-602-27-31.
E-mail address: pourtak@sharif.edu (S.H. Pourtakdoust).

0022-460X/$ - see front matter
doi:10.1016/S0022-460X(03)00779-X

diameter for a desired range increase. On the other hand, for reduced cost of handling and launching operation, efforts have always been made to reduce the missile's structural weight. Obviously, these different requirements lead to a high flexibility missile, for which, dynamic response and vibrational characteristics are of vital importance. The influence of body vibrations on the inertial measuring units (IMU) measurements and the interaction of the control forces on the elastic deformations could cause undesired excitations leading to resonance.

The majority of aeroelastic analysis performed on missiles and rockets have relied on the uniform beam model without axial force (thrust) effect. Whereas large axial force can have a significant influence on the structural natural frequencies and modeshapes, noting that the axial loads in rockets and missiles are usually of compressive nature (namely due to thrust and drag). Bokaian [1] has obtained an analytical characteristic equation for uniform beams under constant compressive axial load and has considered some approximate relations for the buckling load and variation of normalized natural frequency with normalized axial force. Mladenov and Sujiyama [2] have inspected the stability of a rocket modelled as a free–free beam under the thrust action force. They modelled the missile structure with two viscoelastic beams interconnected by a joint that can either be of rotational or shear viscoelastic spring type. Joshi [3] has established a simple method for determining the natural frequencies and modeshapes of a non-uniform beam subjected to rear end thrust. He has also presented the transonic drag effect on the natural frequencies and modeshapes of rockets [4]. Few other researchers have focused on the transverse stability of free–free beams under compressive axial force [5–7]. But the effect of axial force on the vibrational characteristics, flight trajectory and control interactions of guided missiles has not been fully considered.

The complete assessment of elastic vibrational effects on the dynamic behaviour of missiles requires the coupled rigid–elastic equations of motion. Several works involve the derivation of coupled rigid–elastic equations of motion through the Lagrangian approach. Platus [8] has considered the aeroelastic stability of slender spinning missiles by linearizing the equations of motion and using linear aerodynamic formulation. He has observed an instability effect due to structural damping at certain roll rates. Bilimoria and Schmidt [9] have also looked at the complete equations of motion of flexible flight vehicle and evaluated the effect of fluid flow, rotating machinery, wind and spherical rotating earth on the vehicle dynamic behaviour. All the above-mentioned works have employed uniform beam model with no axial force effect. A non-uniform beam model has been utilized in aeroelastic simulation of guided launch vehicles by Pourtakdoust and Assadian [10]. They have done a complete assessment of the influence of various parameters such as engine vibrational forcings, IMU vibrations and location as well as structural damping on the vehicle trajectory and control histories.

This paper investigates the effect of axial force on the aeroelastic and vibrational behaviour of a guided missile. To this end, the governing coupled rigid–elastic equations of motion of Ref. [10] are utilized. In addition a method for the numerical computation of the vehicle structural modeshapes and frequencies is developed, considering variable stiffness, mass and axial force distributions.

By modelling mass consumption, the thrust force effect on the natural frequencies can be determined at various times of flight. Also the mass depletion effect, which can either increase or decrease the natural frequencies in time (depending on the magnitude of thrust), is investigated. The least buckling thrust (associated with the final time of flight) can also be computed, limiting

the maximum allowable thrust. Of course it turns out that the thrust magnitude, which causes structural divergence is much lower than the maximum allowable buckling force.

Time behaviour of controls deflections are considered to evaluate undesirable axial force effects and IMU caused interactions. Usually inclusion of three modes in the simulation provides acceptable precision for displacements [10]. For more realistic results, the engine vibrational forces and measuring devices vibrations are modelled. Since the control system is usually designed assuming rigid body characteristics, the commanded controls could motivate instability once the fundamental natural frequencies decrease below a certain value. By modelling for the engine vibrational forcing in the elastic simulation, one can compute a limit on dynamic stability (in terms of the natural frequency) and in turn, on the maximum thrust tolerable by the structure.

2. Equations of motion

The missile local bending vibrations in y and z directions of the local body axis are modelled based on the method of modal substitution:

$$\mathbf{e}(x,t) = \begin{Bmatrix} 0 \\ \sum_{i=1}^{n} \eta_i(t)\phi_i(x) \\ \sum_{i=1}^{m} \zeta_i(t)\phi_i(x) \end{Bmatrix}, \tag{1}$$

where due to natural symmetry of the vehicle, the modeshapes in the y and z directions have been assumed to be identical and equal to $\phi_i(x)$. The governing equations of motion are developed based on the standard Lagrangian approach:

$$\frac{\mathrm{d}}{\mathrm{d}t}\left(\frac{\partial T}{\partial \dot{\eta}_i}\right) - \frac{\partial T}{\partial \eta_i} + \frac{\partial U}{\partial \eta_i} + \frac{\partial D}{\partial \dot{\eta}_i} = Q_{\eta_i} \tag{2}$$

In Ref. [10] relations for the vehicle total kinetic energy T, potential energy U, and dissipative energy D are presented. The coupled rigid–elastic non-linear equations of motion in final form are given as [10]

$$\dot{U} = \frac{F_x}{m_s} + RV - QW, \tag{3a}$$

$$\dot{V} = \frac{1}{m_s}(F_y + \dot{m}X_{out}R) + PW - RU, \tag{3b}$$

$$\dot{W} = \frac{1}{m_s}(F_z - \dot{m}\,X_{out}Q) + QU - PV, \tag{3c}$$

$$\begin{aligned}\dot{P} = {} & \frac{1}{(I_x + \Sigma(\eta_i^2 + \zeta_i^2))}\big[M_x - \Sigma(\eta_i\ddot{\zeta}_i - \ddot{\eta}_i\zeta_i) - 2P\Sigma(\zeta_i\dot{\zeta}_i + \eta_i\dot{\eta}_i) \\ & + (Q^2 - R^2)\Sigma\,\eta_i\zeta_i + QR\Sigma(\zeta_i^2 - \eta_i^2)\big],\end{aligned} \tag{3d}$$

$$\dot{Q} = \frac{1}{(I + \Sigma\,\zeta_i^2)}\big[M_y + PR(I - I_x) - PR\,\Sigma\,\zeta_i^2 + (\dot{R} - PQ)\Sigma\,\eta_i\zeta_i + 2R\,\Sigma\,\zeta_i\dot{\eta}_i - 2Q\,\Sigma\,\zeta_i\dot{\zeta}_i\big], \tag{3e}$$

$$\dot{R} = \frac{1}{(I + \Sigma\,\eta_i^2)}\big[M_z + PQ(I_x - I) + PQ\,\Sigma\,\eta_i^2 + (\dot{Q} + PR)\,\Sigma\,\eta_i\zeta_i + 2Q\,\Sigma\,\eta_i\dot{\zeta}_i - 2R\,\Sigma\,\eta_i\dot{\eta}\big], \tag{3f}$$

$$\ddot{\eta}_i = Q_{\eta_i} - 2\mu_i\omega_i\dot{\eta}_i + (P^2 + R^2 - \omega_i^2)\eta_i + 2P\dot{\zeta}_i + (-QR + \dot{P})\zeta_i, \tag{3g}$$

$$\ddot{\zeta}_i = Q_{\zeta_i} - 2\mu_i\omega_i\dot{\zeta}_i + (P^2 + Q^2 - \omega_i^2)\zeta_i - 2P\dot{\eta}_i - (\dot{P} + QR)\eta_i. \tag{3h}$$

For solving these equations, external forces and moments are required. These forces consist of gravity, thrust force of missile engine and aerodynamic loads acting on the external surface of the missile body. Gravitational force for an elliptic earth model is obtained as a function of position. Thrust force is due to exhaust gas of the missile, and is easily computed considering distortion and displacement of the exhaust plan due to missile bending vibration.

Vehicle aerodynamic force and moment coefficients per unit length are determined from engineering codes in table look-up form as a function of angle of attack, sideslip, Mach and Reynolds numbers. Due to the vehicle's local bending deflections, the vehicle's local angles of attack and sideslip are determined from the following quasi-static relations:

$$\alpha(x,t) = \tan^{-1}\left(\frac{W_\infty}{U_\infty}\right) + \frac{\dot{e}_z(x)}{U_\infty} + \frac{pe_y(x)}{U_\infty} + \frac{qx}{U_\infty} - e_z'(x), \tag{4a}$$

$$\beta(x,t) = \tan^{-1}\left(\frac{V_\infty}{U_\infty}\right) + \frac{\dot{e}_y(x)}{U_\infty} - \frac{pe_z(x)}{U_\infty} + \frac{rx}{U_\infty} - e_y'(x), \tag{4b}$$

where U_∞, V_∞ and W_∞ are the vehicle's velocity components relative to air speed in the body co-ordinates. The aerodynamic forces and moments per unit length are evaluated as

$$f = q_\infty S_{ref}\bar{C}_f, \tag{4c}$$

$$m = q_\infty S_{ref} L_{ref}\bar{C}_m, \tag{4d}$$

where S_{ref} is the reference area based on vehicle's maximum diameter also, $\bar{C}_f$ and $\bar{C}_m$ are the aerodynamic force and moments coefficients per unit length.

The equations of motion together with the guidance and control algorithm (mentioned below) are integrated in a simulation routine. A proven guidance scheme for the powered phase of launcher applications could be based on the idea of required velocity. The required velocity ($\mathbf{V}_R$) is defined as the burnout velocity, which would provide the desired range when flown ballistically. Using the difference of this velocity and the vehicle instantaneous velocity ($\mathbf{V}$), the velocity to gained ($\mathbf{V}_g = \mathbf{V}_R - \mathbf{V}$) is obtained which is utilized to form the control rate commands [11]:

$$\boldsymbol{\omega}_c^B = k\frac{\mathbf{a}_T^B \times \mathbf{V}_g^B}{\mathbf{a}_T\mathbf{V}_g}, \tag{5}$$

where $\mathbf{a}_T^B$ denotes non-gravitational accelerations and k is a time varying coefficient. In the selected model, the vehicle is controlled via internally actuated control surfaces.

3. Beam model with axial force effect

The Bernoulli–Euler beam bending equation, with axial force effect, is expressed as [1–7]

$$\frac{\mathrm{d}^2}{\mathrm{d}x^2}\left(EI\frac{\mathrm{d}^2\phi}{\mathrm{d}x^2}\right)+\frac{\mathrm{d}}{\mathrm{d}x}\left(N\frac{\mathrm{d}\phi}{\mathrm{d}x}\right)-\rho A\omega^2\phi=0, \tag{6}$$

with the relevant free–free boundary conditions:

$$\frac{\mathrm{d}^2\phi}{\mathrm{d}x^2}=0 \qquad \text{at } x=0,L, \tag{7a}$$

$$\frac{\mathrm{d}}{\mathrm{d}x}\left(EI\frac{\mathrm{d}^2\phi}{\mathrm{d}x^2}\right)+N\frac{\mathrm{d}\phi}{\mathrm{d}x}=0 \qquad \text{at } x=0,L, \tag{7b}$$

where E is Young's module, I the second moment of area, ϕ the transverse modeshape, N the axial force and ρA is the vehicle mass density per unit length. For a non-uniform beam, one needs to resort to a numerical solution of this two point boundary value (TPBV) problem (Eqs. (6) and (7)). However, an analytical solution exists for uniform beams under constant axial compressive load [1]. For numerical solution of this TPBV problem, the missile is divided into several segments of constant density, stiffness and axial force distribution. Thus the modal equation for each segment becomes

$$\frac{\mathrm{d}^4\phi_i}{\mathrm{d}\bar{x}_i^4}+2U_i\frac{\mathrm{d}^2\phi_i}{\mathrm{d}\bar{x}_i^2}-\Omega_i^2\phi_i=0, \tag{8}$$

where $\bar{x}_i$, U and Ω are defined as follows:

$$\bar{x}_i=\frac{x}{L}, \quad 0\leqslant\bar{x}_i\leqslant\bar{l}_i, \quad \bar{l}_i=\frac{l_i}{L}, \tag{9a}$$

$$U_i=\frac{N_iL^2}{2(EI)_i}, \tag{9b}$$

$$\Omega_i^2=\frac{(\rho A)_i\omega^2L^4}{(EI)_i}, \tag{9c}$$

and l_i denotes the ith segment's length. The ith segment uniform parameters can be averaged out over its length. The analytical solution of the Eq. (8) is

$$\phi_i(x)=c_{1_i}\sinh(M_i\bar{x}_i)+c_{2_i}\cosh(M_i\bar{x}_i)+c_{3_i}\sin(N_i\bar{x}_i)+c_{4_i}\cos(N_i\bar{x}_i), \tag{10}$$

where the coefficients M_i and N_i are defined as

$$M_i^2=\sqrt{U_i^2+\Omega_i^2}-U_i, \tag{11a}$$

$$N_i^2=\sqrt{U_i^2+\Omega_i^2}+U_i. \tag{11b}$$

If the missile is divided into n segments, the appropriate boundary conditions will be

$$\frac{d^2\phi_1}{d\bar{x}_1^2} = \frac{d^3\phi_1}{d\bar{x}_1^3} + 2U_1\frac{d\phi_1}{d\bar{x}_1} = 0 \qquad \text{at } \bar{x}_1 = 0, \tag{12a}$$

$$\frac{d^2\phi_n}{d\bar{x}_n^2} = \frac{d^3\phi_n}{d\bar{x}_n^3} + 2U_n\frac{d\phi_n}{d\bar{x}_n} = 0 \qquad \text{at } \bar{x}_n = \bar{l}_n, \tag{12b}$$

where the continuity conditions among the segments require the modeshapes and their slopes, shear force and the bending moments at the connecting nodes to be equal from both sides. Meaning that

$$\phi_i(\bar{l}_i) = \phi_{i+1}(0), \tag{13a}$$

$$\phi_i'(\bar{l}_i) = \phi_{i+1}'(0), \tag{13b}$$

$$\phi_i''(\bar{l}_i) = \phi_{i+1}''(0), \tag{13c}$$

$$\phi_i'''(\bar{l}_i) + 2U_i\phi_i'(\bar{l}_i) = \phi_{i+1}'''(0) + 2U_{i+1}\phi_{i+1}'(0). \tag{13d}$$

Consequently, the 4 boundary relations and $4(n-1)$ continuity conditions could be used for the determination of the $4n$ coefficients c_1 to c_4 (Eq. (10)) over the segments. For a non-trivial solution of the homogeneous set of Eqs. (12) and (13) the determinant of the corresponding coefficient matrix must be zero. This way an algebraic non-linear problem develops which is solved for the unknown variable ω. Then each segment modeshape's coefficients can be computed according to Eqs. (9) and (11). Finally, the vehicle modeshapes are obtained by assembling the segment's modeshapes. This approach of finding the modeshapes and frequencies for non-uniform beams has proven to be very efficient and has generally produced good results even if the vehicle inertial and axial force distribution are highly non-uniform. It needs to be mentioned that since the drag coefficient is usually a function of Mach numbers developing in flight, they complicate the offline computations of modeshapes and frequencies. Thus the drag effect was initially not considered in the modal computations. But later in the study, it was found that higher thrust values cause higher speeds and higher drag, in such a way that the acceleration remains approximately constant. This in turn means that the axial force distribution would not change much in flight for the case under study. Otherwise drag distribution in flight must be similarly taken into account.

4. Results

One of the key purposes of this study has been to determine the effect of thrust force on the vibrational and aeroelastic behaviour of elastic missiles. For this analysis, one needs to initially solve the free–free beam eigenvalue problem at various points of flight to determine the vehicle modal characteristics in time. And subsequently investigate the aeroelastic as well as vibrational characteristics of the missile dynamic through a non-linear simulation. In Fig. 1 a schematic diagram of the simulation routine is provided. As can be seen from this diagram, the equations of motion are noted as *Missile Dynamics*, where aeroelastic phenomena is created through interactions of the inertial, elastic, aerodynamic, thrust and control forces. A complete simulation

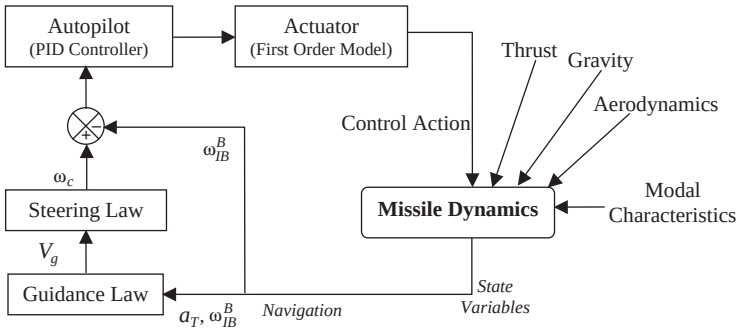

Fig. 1. Schematic diagram for the aeroelastic simulation package.

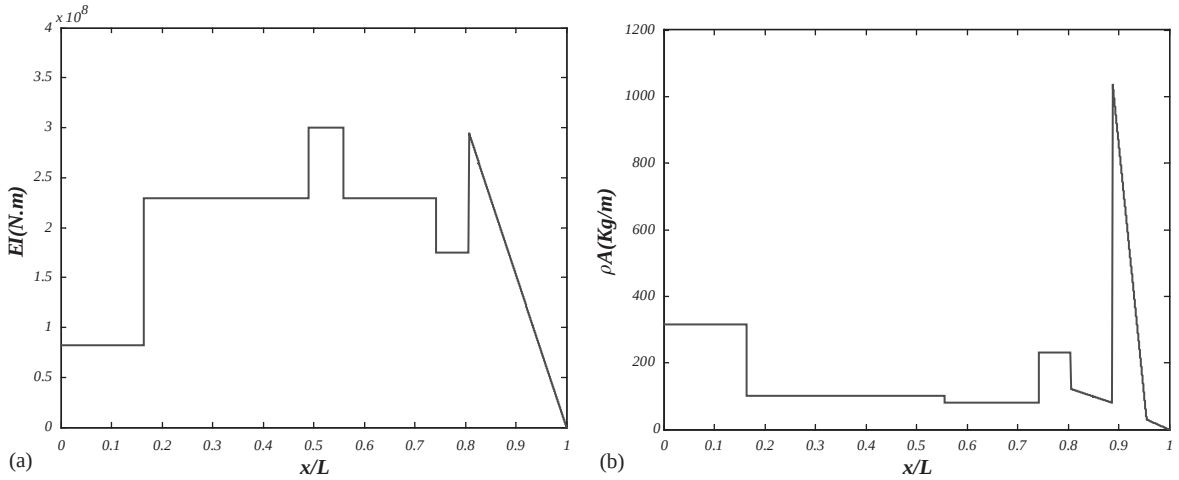

Fig. 2. (a) Distribution of bending stiffness at final time of flight; (b) distribution of mass density at final time of flight.

program has been developed in-house in the C^{++} environment. The vehicle non-linear equations of motion are time integrated using a fourth order forward Runge–Kutta algorithm.

As described before, in order to solve the eigenvalue problem, the vehicle is divided into several segments, in which EI, ρA and N distributions are uniform. Note that even with uniform stiffness and density distributions over some certain segment, axial force distribution will not necessarily be uniform due to accelerated motion of the missile. Joshi [3] has inspected the eigenvalue convergence problem with an increasing number of segments and concluded that division of a missile into more than eight segments yields no more effects on the modal results. In this study the missile is divided into 10 segments. Figs. 2a and b show axial variations of EI and ρA distributions at the end of power phase.

As may be intuitively obvious, the thrust force reduces the natural frequencies. On the other hand mass depletion increases it. Fig. 3 shows variation of the fundamental mode frequency with increasing thrust at some selected times of flight. Since at the beginning of flight the missile has its maximum mass, it turns out that for small thrust magnitudes, natural frequencies are low and

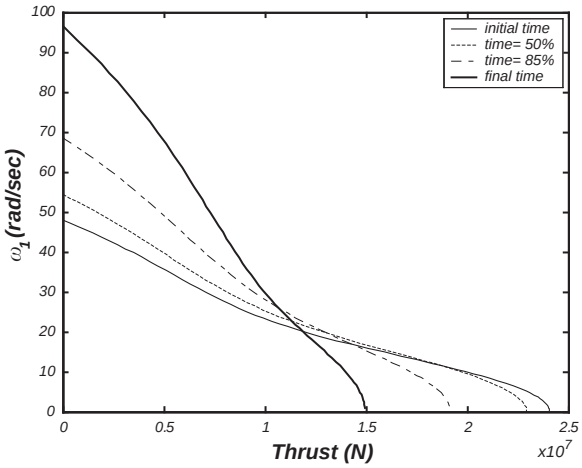

Fig. 3. Effect of thrust modelling on the natural frequency of first mode at a few selected times of flight.

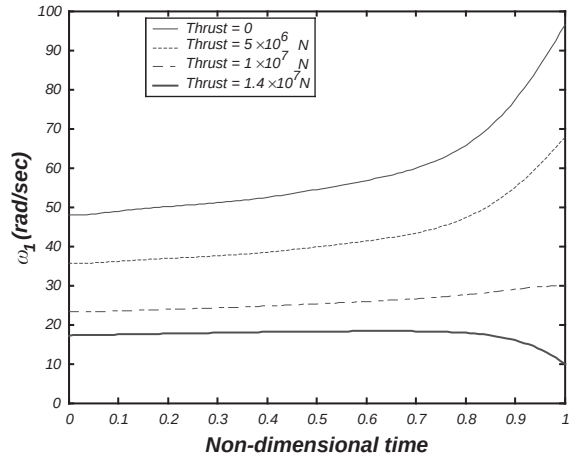

Fig. 4. Effect of thrust magnitude on the natural frequency of the first mode.

increase in time (Fig. 4). But for higher thrust magnitudes the mass depletion leads to increased acceleration and axial force distribution, which in turn inhibits the natural frequencies from increasing. Figs. 3 and 4 show this trend of natural frequencies reducing in time for high thrust magnitudes. Note that zero natural frequency corresponds to critical buckling thrust. Also at the end of the power phase (point of minimum mass), buckling thrust is less than at other times and therefore is the limiting maximum allowable thrust. To see the effect of thrust on the modeshapes, a nominal thrust magnitude of 1×10^7 N was selected and its corresponding fundamental modeshape was compared with that of zero thrust (i.e. thrust effect not modelled for modal computations). Thrust effect is seen to reduce the magnitude of the modeshape adjacent to the thrust point of action (vehicle rear end) (Fig. 5), and because of modeshape normalization, the

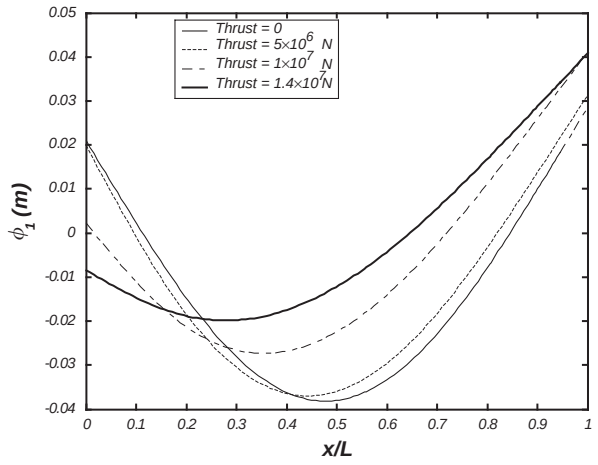

Fig. 5. Effect of thrust magnitude on the first modeshape at final time of flight.

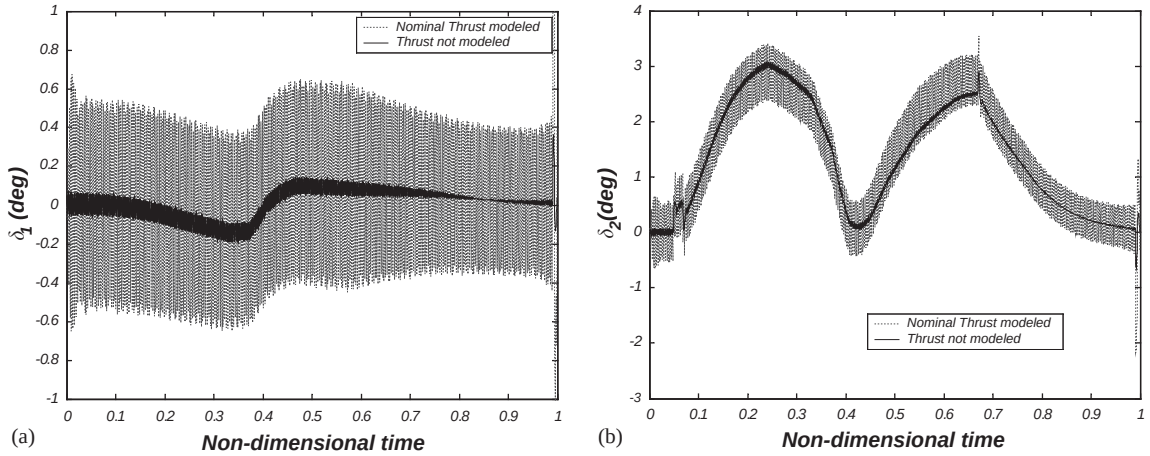

Fig. 6. (a) Effect of thrust modelling on the yaw control deflections; (b) effect of thrust modelling on the pitch control deflections.

magnitude of the modeshape increases near the missile nose. This phenomenon, in turn, motivates IMU induced vibrations considering the forward location of the IMU. In Ref. [10] it was found that IMU location in the aft portion of vehicle could lead to dynamic instability. Increasing thrust causes a backward shift in the extremum point of the fundamental modeshape curve, allowing a larger margin of safety for the IMU induced vibration.

For analysis of thrust modelling effect on controls, the internal control deflections were considered. Four control surfaces in the exhaust nozzle supply the missile control power. Since they act symmetrically for the non-spinning missile, only two controls' time histories are presented in Fig. 6.

To see the effect of high frequency exciting forces acting on the vehicle in actual flight, a harmonic forcing function:

$$F_{excite} = A \sin(\omega_{excite} t) \tag{14}$$

is utilized representing the engine related excitations at a distance about $0.17L$ from the missile end, where, A is the amplitude and ω_{excite} is the forcing function frequency, which are selected as 1000 N and 20 rad/s, respectively. It was found through simulation that with this forcing function present, the vehicle is guided poorly and in some conditions destabilizes completely. A reason for this behaviour could be due to rigidity assumption usually made during the control system design. This problem can be circumvented through a low-pass filter on the IMU avoiding high frequency fluctuations in its outputs. The missile bending (Fig. 7) shows a quasi-static behaviour influenced by the aerodynamic forces. Under these conditions, it turned out that if the fundamental frequency was less than 5 rad/s, structural divergence would occur. This means that inclusion of the exciting force with a thrust magnitude greater than 1.2×10^7 N, leads to complete instability, even though this value of thrust is less than the buckling thrust of 1.5×10^7 N computed at the end of power phase.

In Fig. 6 control deflections are compared with/without thrust modelling effect. It can be seen that the magnitude of control fluctuations increases once thrust effect is considered in modal computation.

Fig. 6 shows that the intensity of the control fluctuations increases by modelling the thrust effect, and that their mean values are shifted compared with no thrust effect. This is specially noticeable for control surface 2 shown in Fig. 6b. By reduction of the magnitude of bending stiffness the bending displacements increase and deform more especially at the exhaust plane, where controls are located which consequently causes the control actions to shift up or down depending on the displacement direction.

It turns out that for the problem under study the displacements rapidly increase once thrust magnitude becomes lower than 1.2×10^7 N, so that dynamic–elastic coupling intensifies, ultimately destabilizing the vehicle.

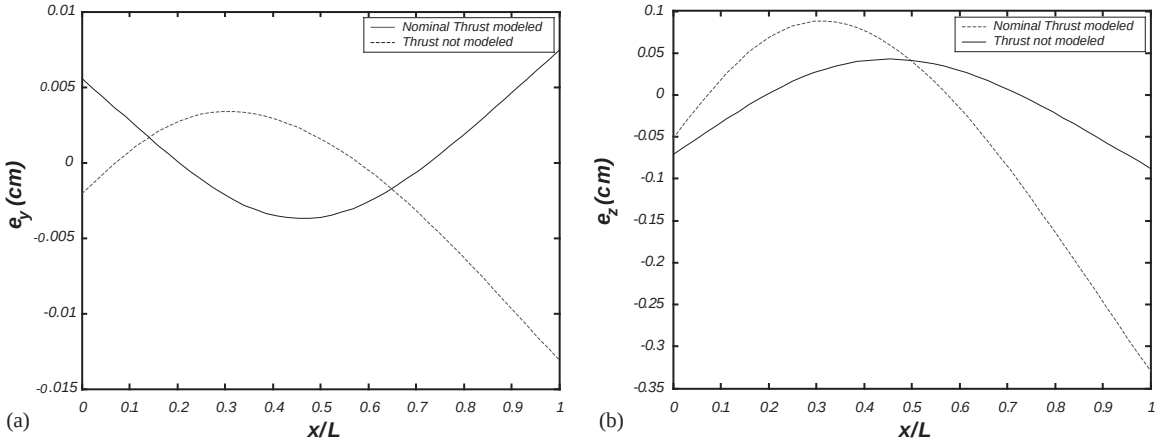

Fig. 7. (a) Effect of thrust modelling on the y direction bending shape at mid-time of flight; (b) effect of thrust modelling on the z direction bending shape at mid-time of flight.

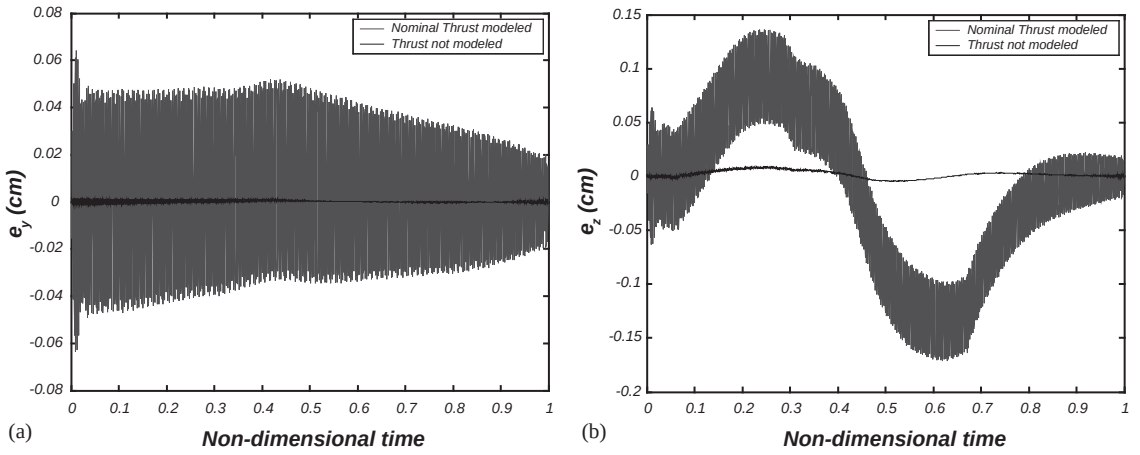

Fig. 8. (a) Effect of thrust modelling on the y direction bending displacement at the IMU position; (b) effect of thrust modelling on the z direction bending displacement at the IMU position.

In Fig. 7, missile displacements in the y and z directions at mid-time of flight are compared with and without thrust modelling effect. The total thrust modelling effect on the bending displacements is of course due to both the modeshape changes as well as the natural frequency reduction. In Fig. 8 the vehicle displacements at the IMU location is shown with time, verifying the significance of thrust modelling in modal computation of an elastic vehicle. As can be seen oscillation intensity and bending behaviour are completely modified once the thrust effect is modelled.

5. Concluding remarks

The methodology presented in this study allows for a more realistic simulation of a flexible missile. Inclusion of the thrust effect in the non-uniform beam model renders more accurate modal results needed for an elastic simulation. Influence of the thrust modelling effect and exciting forces on the vehicle vibrational characteristics, control actions and flight trajectory are investigated.

Depending on the magnitude of thrust as an axial force, it can play a vital role in natural frequency reduction and modeshape changes of flexible missiles. Imposing engine vibrational forces and modelling the fluctuations picked up by IMU in the guidance/control system causes high fluctuation of the control deflections and motivates missile bending vibrations. IMU location is important when adverse interaction with the local missile vibration occurs. Also it turned out that modelling for the thrust effect reduces the natural frequencies and increases the modeshape value at the IMU location, in turn intensifying structural vibrations. Mass consumption could increase or decrease vehicle fundamental frequency depending on the thrust magnitude.

Appendix A. Nomenclature

η_i, ζ_i	ith mode generalized co-ordinates
$\phi_i(x)$	ith modeshape

$\mathbf{e}$	vehicle local displacement vector
U, V, W	missile velocity vector
P, Q, R	missile angular velocity vector
F_x, F_y, F_z	external forces
M_x, M_y, M_z	external moments
ω_i	ith mode natural frequency
Q_{η_i}, Q_{ζ_i}	ith mode generalized forces
m_s	vehicle structural mass
X_{out}	distance from the hot gases exit plane to the burning area
$\dot{m}$	fuel and oxidizer mass flow rate
μ_i	critical damping ratio
$\mathbf{V}_R$	required velocity
$\mathbf{V}_g$	velocity to be gained
ω_c	rate command
$\mathbf{a}_T$	vehicle non-gravitational acceleration vector
$\alpha(x, t)$	local angle of attack
$\beta(x, t)$	local angle of sideslip
$U_\infty, V_\infty, W_\infty$	missile velocity vector relative to surrounding air
q_∞	dynamic pressure
S_{ref}	reference area
L_{ref}	reference length
$\bar{C}_f, \bar{C}_m$	aerodynamic force and moments coefficients per unit length
ρA	vehicle mass density per unit length
EI	vehicle bending rigidity
$\bar{x}_i, \bar{l}_i$	non-dimensional co-ordinate and length of ith segment
U_i	non-dimensional axial force of ith segment
Ω_i	non-dimensional natural frequency of ith segment
F_{excite}	harmonic exciting force

References

[1] A. Bokaian, Natural frequencies of beam under compressive axial loads, *Journal of Sound and Vibration* 126 (1) (1988) 49–65.

[2] K.A. Mladenov, Y. Sujiyama, Stability of a jointed free–free beam under end rocket thrust, *Journal of Sound and Vibration* 199 (1) (1997) 1–15.

[3] A. Joshi, Free vibration characteristics of variable mass rocket having large axial thrust/acceleration, *Journal of Sound and Vibration* 187 (4) (1995) 727–736.

[4] A. Joshi, Transonic drag effect on vibrating characteristics of single-stage space vehicles, *Journal of Spacecraft and Rockets* 33 (2) (1996) 308–309.

[5] K. Sato, On the governing equation for vibrating and stability of a Timoshenko beam: Hamilton's principle, *Journal of Sound and Vibration* 145 (2) (1991) 338–340.

[6] M.J. Maurizi, P.M. Belles, General equation of frequencies for vibrating uniform one-span beams under compressive axial loads, *Journal of Sound and Vibration* 145 (2) (1991) 345–347.

[7] G.C. Nihous, On the continuity of boundary value problem for vibrating free–free straight beams under axial loads, *Journal of Sound and Vibration* 200 (1) (1997) 110–119.
[8] D.H. Platus, Aeroelastic stability of slender, spinning missiles, *Journal of Guidance, Control and Dynamics* 15 (1) (1990) 144–151.
[9] K.D. Bilimoria, D.K. Schmidt, Integrated development of the equation of motion for elastic hypersonic flight vehicle, *Journal of Guidance, Control and Dynamics* 18 (1) (1995) 73–81.
[10] S.H. Pourtakdoust, N. Assadian, Aeroelastic simulation of guided missile, M.S. Project, Sharif University of Technology, 2001.
[11] R.H. Battin, *An Introduction to Mathematics and Methods of Astronautics*, Education Series, AIAA, New York, 1987.